International Journal on Robotics, Automation and Sciences

Effects of Various Earth Grid Configurations on Ground Potential Rise Caused by Lightning Strike

Febby Purnama Madrin, Hafild Widyaputera, Eko Supriyanto*, Zulkurnain Abdul Malek, Mohammad Akmal Abu Taib, and Muhammad Faudzi Mohd Yasir

***Abstract*— Ground Potential Rise (GPR) caused by lightning strike is a potential hazard for electrical equipment inside an oil and gas refinery plant. In order to mitigate the risk, horizontal grounding grid is applied. The best mitigation is to install a grounding grid with mesh size as small as possible. This condition requires a high cost. In order to obtain the optimal mesh size, a series of simulation of a grounding grid with mesh size variations on GPR caused by lightning strike has been carried out. CDEGS software was used to observe the GPR with various mesh size from 6.5 x 6.5 m to 20 x 20 m. Simulation results show that the maximum transient GPR rises as the grounding grid mesh size is increased, while the GPR distribution throughout the grounding grid area does not change much for different mesh sizes. In the other hand, decreasing the grid size would mean that more conductors are required, hence the cost would increase accordingly. The result shows that grid sizes from 6.5 x 6.5 m up to 20 x 20 m have no significant difference in term of GPR. In term of cost, 10 x 10 m does not show significant difference with 20 x 20 m, on the other hand, there is a significant difference for grid sizes 1 x 1 m to 10 x 10 m. From the results, grid sizes between 10 x 10 m up to 20 x 20 m are still applicable as stated in Petronas Technical. To comply with proper GPR value, additional protection devices are needed to protect the electrical equipment from potential damage.**

Keywords*— *Ground Potential Rise, Grounding Grid, Mesh Size

I. Introduction

When a plant is struck by direct or indirect lightning, the lightning current will flow to the earth. On its way, the lightning current passes through the earthing or grounding network. This occurrence will lead to the change of the earth potential, which furthermore will cause damage to the site or plant [1].

This potential change, which is known as the Ground Potential Rise (GPR) might occur since the grounding electrode itself has resistivity. The respective GPR will develop across the grounding electrodes with respect to remote earth [2]. Every electrical equipment which is located in or near the plant area might be damaged because the ground potential actually rises to thousands of volts above the remote earth potential [3]. However, many simulation works and experiments were done in the past on the GPR occurrence with various methods of testing and grounding system configurations [4-12].

II. Ground Potential Rise

GPR is defined as the maximum electrical potential that a ground electrode may attain relative to a distant grounding point assumed to be at the potential of remote earth [13]. This voltage, GPR, is equal to the maximum grid current multiplied by the grid resistance. GPR can be harmful to electrical equipment when a connection through two different appliances allows the current from lightning strike to flow through the equipment instead of flowing through the ground.

The GPR at the point of current injection is given as in (1) [14].

$$GPR = I_G \times R_G \qquad (1)$$

I_G = Maximum grid current

R_G = Total resistance of a grounding system

*Corresponding author. Email : eko@utm.my ORCID: 0000-0002-6766-793X

Febby Purnama Madrin is with E-Life Solution PLT, Johor Bahru 81310, Malaysia and School of Biomedical Engineering and Health Sciences, Faculty of Engineering, Universiti Teknologi Malaysia (e-mail: febby@elife-solutions.com)

Hafild Widyaputera is with E-Life Solutions PLT, Johor Bahru, Malaysia (email: hafild.dimas@gmail.com).

Eko Supriyanto is with Advanced Diagnostics and Progressive Human Care Research Group, IJN-UTM Cardiovascular Engineering Center, Institute of Human Centered Engineering, School of Biomedical Engineering and Health Sciences, Faculty of Engineering, Universiti Teknologi Malaysia 81310 Johor Bahru, Malaysia (email: eko@utm.my)

Zulkurnain Abdul Malek is with Institute of High Voltage and High Current, Universiti Teknologi Malaysia 81310 Johor Bahru, Malaysia (email: zulkurnain@utm.my)

Mohammad Akmal Abu Taib and Muhammad Faudzi Mohd Yasir are with Petroliam Nasional Berhad, Malaysia (email: akmal_abutaib@petronas.com)

International Journal on Robotics, Automation and Sciences (2019) 1:11-18
https://doi.org/10.33093/ijoras.2019.1.2
Manuscript received: 12 Jun 2019 | Revised: 25 Sep 2019 | Accepted: 20 Oct 2019 | Published: 13 Nov 2019
Published by MMU PRESS. URL: http://journals.mmupress.com/ijoras

Although various standards consider the safety of human being against the step and touch voltages on a grounding facility, as in IEEE standard 80-2000 [15] and IEC 62305-(1-4) [16-19], there is yet enough attention on considering the safety of the power system, which may have a huge relationship with the GPR. Materials with high resistivities, such as gravel, cement, and crushed-rock, usually cover the top layer of the grounding system to improve the step and touch voltages limitation. The other way around is by increasing the density of the horizontal conductors in the grounding system [20]. In China, the maximum limit of allowable GPR of substation grounding system is only 5 kV [20].

III. Grounding Grid Configuration Variations

In this paper, variations of mesh size are implemented for the grounding. The size of the mesh is changing in each case while maintaining the homogenous rectangular shape in the grounding grid. Consequently, grounding grid configuration with smaller mesh size will require a longer length of the conductor, while bigger mesh size will require a lesser amount of grounding conductor.

As mentioned before, improving the conductor density by decreasing the mesh size will sufficiently improve the grounding performance on dealing with step and touch voltages. A rectangular grounding grid can be divided into various numbers of mesh size. As the mesh size decreased, the conductor span will eventually get smaller. Furthermore, the total length of a conductor will increase, and as this occurs, the impulse grounding resistance will decrease, which is confirmed by Zeng, shown in the graph on Figure 1 [21]. In Figure 1, ρ is the earth resistivity.

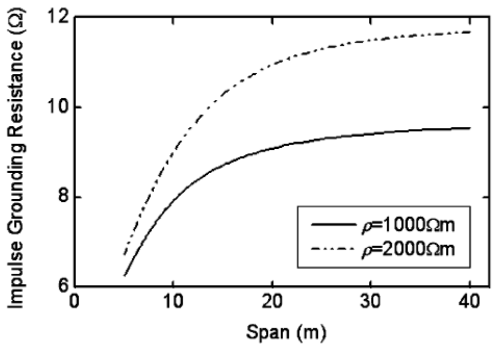

FIGURE 1. Influence of the conductor spans on impulse grounding resistance.

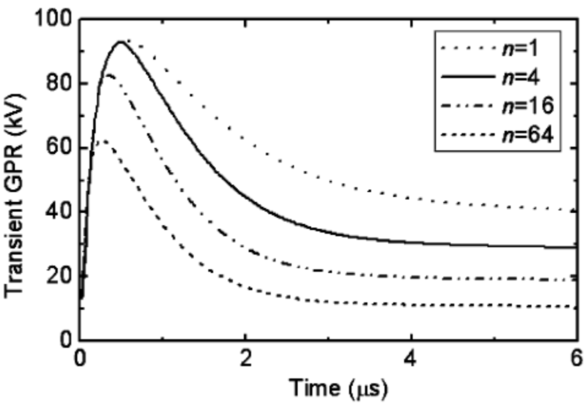

FIGURE 2. Influence of the conductor spans on the maximum transient GPR.

In his experiments, Zeng injected an impulse current, with a 2.6/50 µs and amplitude I_m of 10 kA to the grounding grid. In Figure. 2, n is the number of individual grid squares inside the bigger grounding grid square. For example, in a 10 x 10 m grounding grid, if the individual grid size is 10 x 10 m, then n=1. If the individual grid size is 5 x 5 m, then n=4. If the individual grid size is 2 x 2 m, n=25. The result shows that lesser impulse grounding resistivity will eventually produce significantly smaller transient GPR for n = 4, n = 16, and n = 64. For n = 1, the difference with n = 4 is not drastic, and the graph is sloping rather gently. This is due to the fact that the impulse grounding resistivity is not reduced significantly for n = 1 and n = 4. In the opposite, it drops down from n = 4 onwards, causing the maximum transient GPR to decline significantly. Therefore, according to this experiment, having a 10 m span between the conductors will not effectively reduce the maximum transient. For simplicity, we may apply a higher span which requires lesser conductors and still gets a similar value of maximum transient GPR.

IV. Methods and Simulation Parameters

As mentioned before, the modelling and simulation are to be carried out by using CDEGS software. Figure 3 depicts how the grounding grid in the plant is modelled in the software.

FIGURE 3. Diagram of grounding grid of the plant (represented by 200 x 200 m area).

Later on, the soil profile, grounding grid system parameters, lightning characteristics, and striking point are all inputted to the simulation model. The lightning model that is used in this simulation is defined in the standard made by IEC, as in Figure. 4 [22]. The rise time of the lightning is about 10 µs, while the fraction time is 350 µs. Secondly, the current magnitude induced by lightning is 200 kA. Additionally, the striking point is located in the center of the grounding grid, 100 m in distance from each side. The lightning parameters in the simulation are shown in TABLE I.

There are five variations of mesh size, from 6.5 by 6.5 m to 20 by 20 m, as stated in Table 2.

The simulation results of current grounding grid system with mesh size of 10 m by 10 m are to be compared with the other mesh sizes to find out the most optimum mesh size for the oil and gas refinery plant.

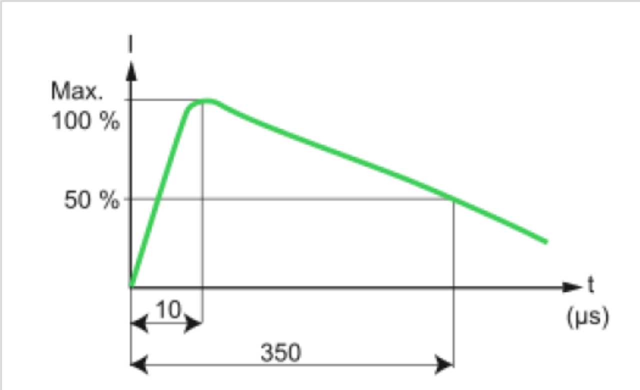

FIGURE 4. Lightning, IEC Std. 61643-11.

TABLE 1. Lightning Strike Parameters.

Parameter	Value
Type	Standard
Rise Time (µs)	10
Maximum Magnitude (A)	200,000
Fraction of Maximum Magnitude (p.u.)	0.5
Fraction Time (µs)	350

TABLE 2. Grounding mesh size variation.

Simulated grounding area (m^2)	Mesh size (m^2)	Number of ground rods
200 x 200	6.5 x 6.5	36
	7.5 x 7.5	36
	10 x 10	36
	15 x 15	36
	20 x 20	36

V. Result and Analysis

Overall, the results are divided into two main subjects, which are the maximum transient GPR and the GPR distribution throughout the grounding grid area.

A. Maximum transient GPR

The effects of different mesh sizes on GPR waveforms were measured. From Figure. 5 to Figure. 9 show the maximum transient GPR distribution for mesh sizes from 20 m by 20 m to 6.5 m by 6.5 m mesh. Table 3 summarizes the maximum transient GPR for all mesh size variations, while the overall trend is shown in Figure 10.

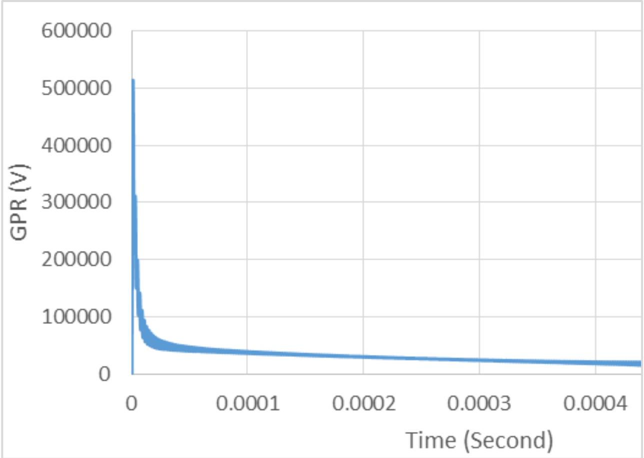

FIGURE 5. Maximum transient GPR for 6.5 x 6.5 m mesh size.

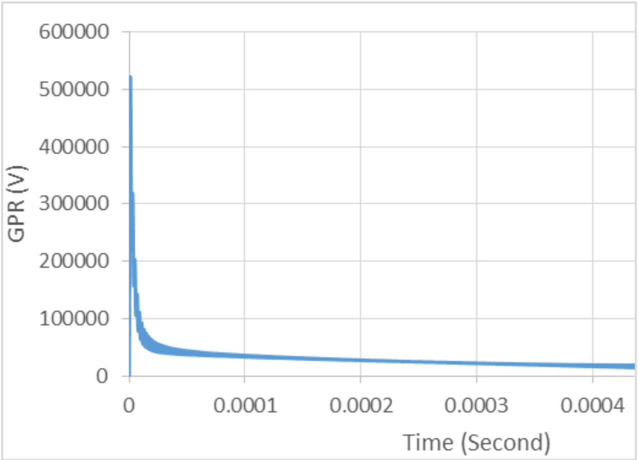

FIGURE 6. Maximum transient GPR for 7.5 x 7.5 m mesh size.

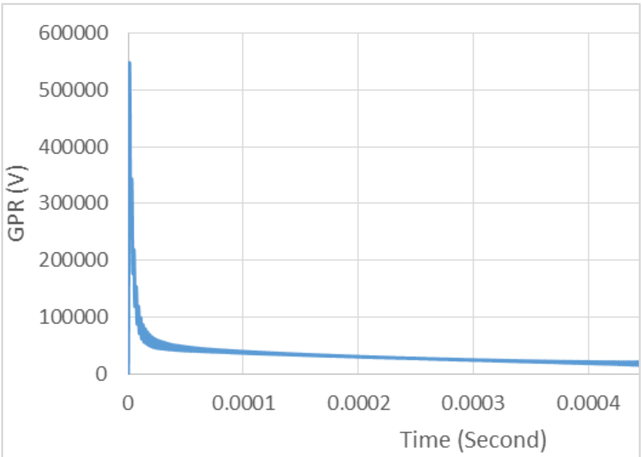

FIGURE 7. Maximum transient GPR for 10 x 10 m mesh size.

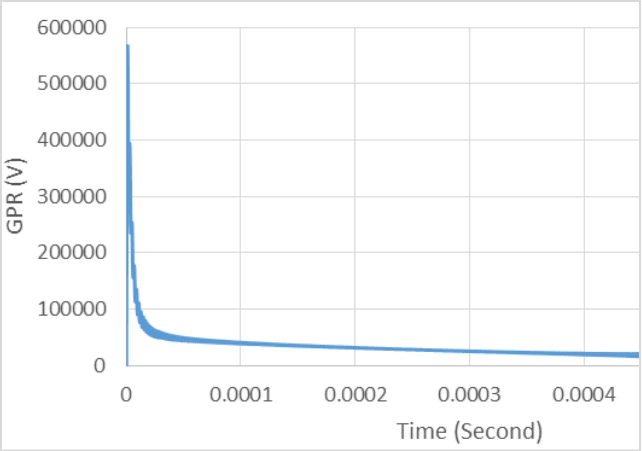

FIGURE 8. Maximum transient GPR for 15 x 15 m mesh size.

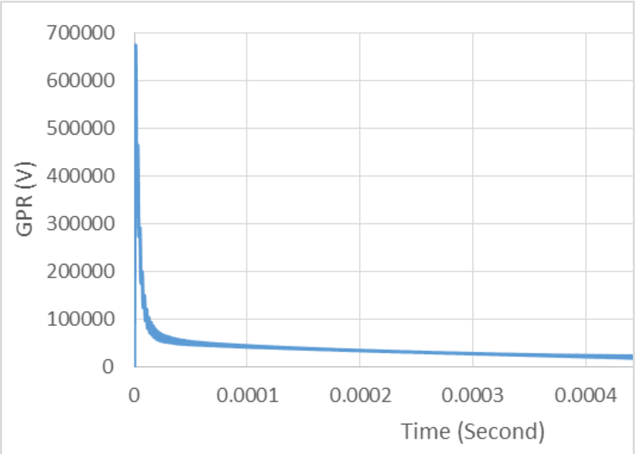

FIGURE 9. Maximum transient GPR for 20 x 20 m mesh size.

TABLE 3. Maximum GPR for various mesh size.

Mesh size	Area (m)	Maximum voltage (V)
6.5 x 6.5	200 x 200	510,806
7.5 x 7.5	200 x 200	518,493
10 x 10	200 x 200	544,087
15 x 15	200 x 200	559,078
20 x 20	200 x 200	663,613

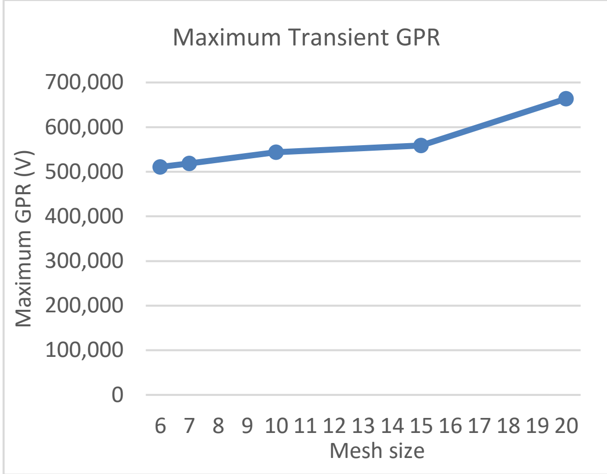

FIGURE 10. Maximum transient GPR for various mesh size.

The graphs show similar results with the experiments conducted by Rong Zeng et al. [21], even under different conditions and simulation parameters. Grounding grid with higher conductor density eventually produced less maximum transient GPR. In a 6.5 x 6.5 m grounding grid, after travelling for 20m, the induced lightning current dispersed into 28 different way, and some part of it to earth. Meanwhile, in a 10 x 10 m grounding grid, the current dispersed into 20 different ways, and in 20 x 20 m grounding grid, they have only finished travelling 20m in 4 different ways. Due to this fact and the involvement of current already traveled to the ground, the graph would be non-linear. However, the drops were insignificant, as both of them still potentially might cause severe harm on electronics devices.

B. GPR distribution throughout grounding grid

From Figure 11 to Figure 15 depict the GPR distribution throughout the grounding grid area. The graphs are 3D charts which are rotated to bird's eye point of view, and each point in the x and y axis stands for each of the horizontal conductors.

Furthermore, each different color in the graph indicates a certain range of voltage level, which is stated in the information below each graph.

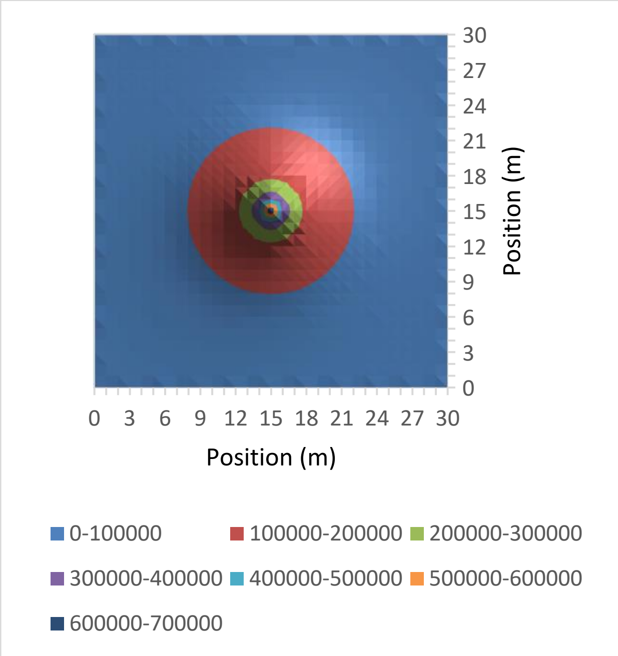

FIGURE 11. 6.5 x 6.5 m mesh GPR distribution (Various color indicates voltage value).

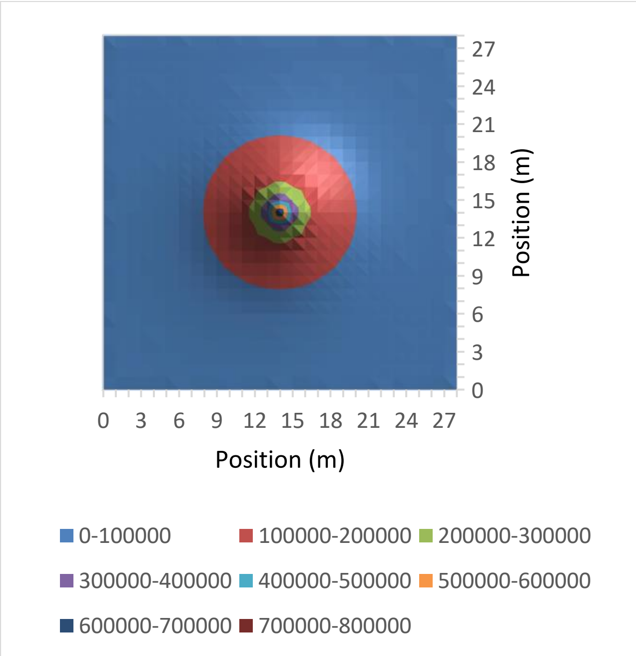

FIGURE 12. 7.5 x 7.5 m mesh GPR distribution (Various color indicates voltage value).

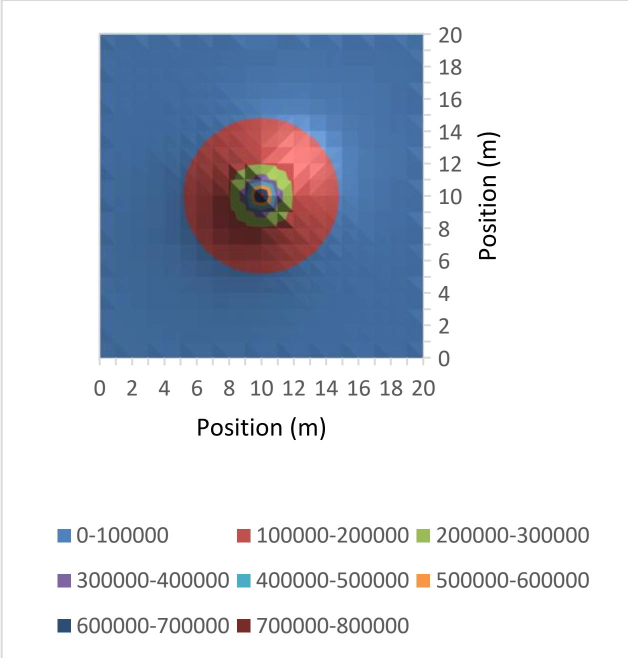

FIGURE 13. 10 x 10 m mesh GPR distribution (Various color indicates voltage value).

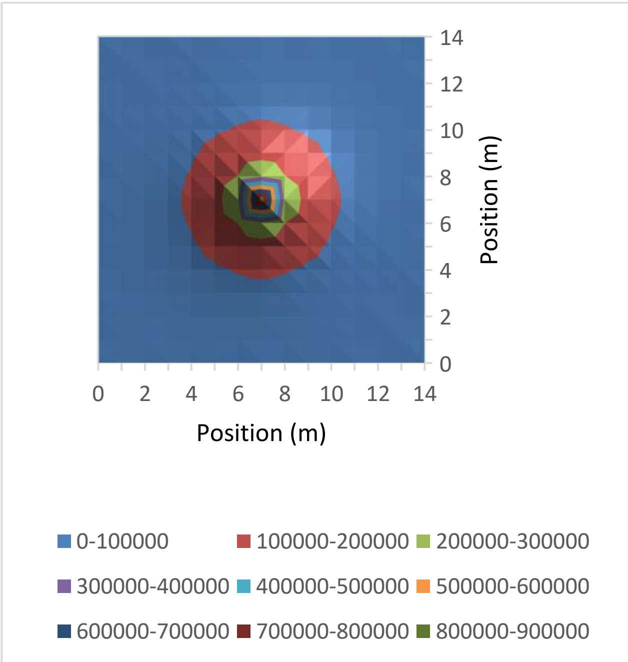

FIGURE 14. 15 x 15 m mesh GPR distribution (Various color indicates voltage value).

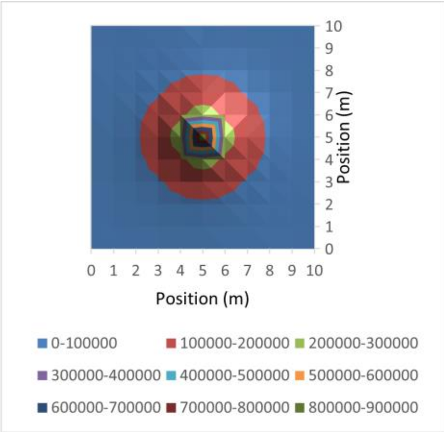

FIGURE 15. 20 x 20 m mesh GPR distribution (Various color indicates voltage value).

Typically, the GPR is smaller as the point of observation stand farther from the lightning striking point. The highest GPR level is to be found on the striking point. However, the GPR actually increases slightly by a very small amount when it reaches the edge of the grounding grid. The increase is less than 1 kV. This is due to the limitation of the option for distributing the lightning current on the last conductor. Among all of the graph results, there is no significant difference in the GPR distribution.

The border between the red-colored area and the blue-colored area is where the GPR reaches 100 kV. As it seems, there is no significant difference among all the mesh size variations. The summarization of this radius perimeter of 100 kV GPR is shown in Table 4 and Figure 16.

TABLE 4. 100 KV Radius Summarization.

Mesh size	Area (m)	Distance (m)
6.5 x 6.5	200 x 200	45.5
7.5 x 7.5	200 x 200	45.75
10 x 10	200 x 200	48
15 x 15	200 x 200	52.5
20 x 20	200 x 200	58

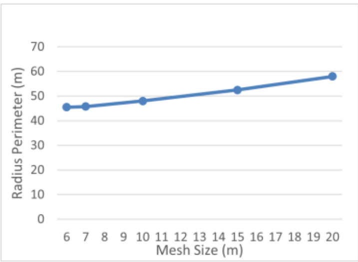

FIGURE 16. 100 kV GPR radius summarization.

Figure 16 shows that grounding grid with smaller mesh size has a smaller area of where the GPR surpass 100 kV. However, all the grounding grid system variations are still not capable to limit the GPR properly, if the site is to be struck by 200 kA lightning.

However, as shown in Figure 17, the total conductor lengths from 1 x 1 m to 10 x 10 m are different exponentially. On the other hand, there is no significantly different for mesh sizes from 10 x 10 m to 20 x 20 m. From this situation, it is recommended to have a mesh size between 10 x 10 m and 20 x 20 m.

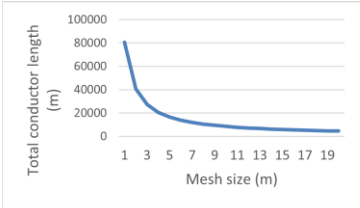

FIGURE 17. Total conductor length of 1 x 1 m up to 20 x 20 m mesh size.

The configuration of the electrical equipment connection very much defines how the protection device should be installed. The ground potential difference which leads to equipment damage may happen on separate ground electrode systems. Hence, a single point grounding is a must to prevent equipment damage.

Aside from the single grounding system, surge protection should be added on electrical equipment. This device works to limit transient voltages and divert surge current. If somehow a lightning strike induces a massive amount of current and causes an overvoltage in the supply line, the excessive current will be distributed to earth through the surge protection device, which is connected in parallel with the load.

VI. Conclusion

The rectangular grounding grid system in an oil and gas refinery plant with variations of mesh size has been modelled in order to study the effects of 200 kA lightning strike on GPR. The simulation results show that grounding grid with 6.5 x 6.5, 7.5 x 7.5, 10 x 10, 15 x 15, and 20 x 20 mesh size has 45.5, 45.75, 48, 52.5, and 58 m of radius where the GPR reaches 100 kV respectively.

Since in most cases the GPR limit is only about 5 kV, there is no significant difference on the maximum transient GPR level and GPR distribution of various mesh size grounding grid system. According to the data, grounding grid with smaller mesh size has less area with GPR of 100 kV, if injected with 200 kA lightning.

GPR is smaller as the point of observation stands farther from the lightning striking point. When the injected current reaches the edge of the grounding grid, the GPR increases slightly by a very small amount, less than 1 kV, as there is a limited option for distributing the lightning current on the last conductor.

Based on these results, there is no need for changing the ground grid system configuration in order to reach optimum performance on facing GPR from lightning strike.

Acknowledgment

This work was supported in part by the Ministry of Higher Education Malaysia, Universiti Teknologi Malaysia under Grant GUP 16H82, E-Life Solutions PLT, and Petroliam Nasional Berhad, Malaysia.

Author Contributions

Febby Purnama Madrin: Conceptualization, Methodology, Validation, Writing – Original Draft Preparation;

Hafild Widyaputera: Literature Review;

Eko Supriyanto: Project Administration, Supervision, Writing – Review & Editing;

Zulkurnain Abdul Malek: Data Curation, Validation;

Mohammad Akmal Abu Taib: Data Curation, Simulation;

Muhammad Faudzi Mohd Yasir: Validation, Writing – Review & Editing.

Conflict of Interests

No conflict of interests was disclosed.

Ethics Statements

Our research work follows The Committee of Publication Ethics (COPE) guideline. https://publicationethics.org.

References

[1] J. Liu, L. Cheng and Z. Qi, "Impact of secondary effect of earth potential rise caused by lightning strike on lightning introduction port in base station," *IEEE 2014 International Conference on Lightning Protection (ICLP)*, pp. 188-191, 2014.
DOI: https://doi.org/10.1109/ICLP.2014.6973118

[2] P. H. Pretorius, "On ground potential rise presented by small and large earth electrodes under lightning conditions," IEEE AFRICON, pp. 1055-1060, 2017.
DOI: https://doi.org/10.1109/AFRCON.2017.8095628

[3] D. Haluza, "Lightning, ground potential rise, and electrical damage; protecting wayside equipment on the MTA Long Island Rail Road," *Proceedings of the 1996 ASME/IEEE Joint Railroad Conference*, pp. 111-135, 1996.
DOI: https://doi.org/10.1109/RRCON.1996.507966

[4] S. Zhen, W. Jianguo, Q. Xiushu, X. Nianwen, F. Chunhua and C. Junjie, "Observation of lightning current and ground potential rise in artificially trigged lightning experiment," *IEEE International Conference on High Voltage Engineering and Application*, pp. 277-280, 2008.
DOI: https://doi.org/10.1109/ICHVE.2008.4773927

[5] J. Yang, J. G. Wang, Y. Zhao, Q. L. Zhang, T. Yuan, Y. J. Zhou and G. L. Feng, "Observation of ground potential rise caused by artificially-triggered lightning," *IEEE 2010 Asia-Pacific International Symposium on Electromagnetic Compatibility*, pp. 1297-1300, 2010.
DOI: https://doi.org/10.1109/APEMC.2010.5475745

[6] T. Thanasaksiri, "Ground potential rise from lightning overvoltage in communication station," *IEEE 2008 5th International Conference on Electrical Engineering/Electronics, Computer, Telecommunications and Information Technology*, vol. 2, pp. 905-908, 2008.
DOI: https://doi.org/10.1109/ECTICON.2008.4600577

[7] T. Chen, H. Liu, D. Hu, X. Liu, T. Xu, X. Yang and L. Ji, "Shell circulating current and transient ground potential rise in 220 kV GIS," *The Journal of Engineering*, no. 13, pp. 2555-2558, 2017.
DOI: https://doi.org/10.1049/joe.2017.0788

[8] S. T. Sobral, J. A. Barbosa, J. V. Nunes, E. Chinelli, A. F. Netto, V. S. Costa and J. H. Campos, "Ground potential rise characteristics of urban step-down substations fed by power cables-a practical example," *IEEE Transactions on Power Delivery*, vol. 3, no. 4, pp. 1564-1572, 1988.
DOI: https://doi.org/10.1109/61.193956

[9] X. Liu, X. Lv, X. Sun, T. Wang, S. Wang, P. Yu, Y. Pei, L. Ji, D. Hu and H. Liu, "Research on 220kV GIS enclosure circulation and temporary ground potential rise," *IECON 2017-43rd Annual Conference of the IEEE Industrial Electronics Society*, pp. 398-404, 2017.
DOI: https://doi.org/10.1109/IECON.2017.8216071

[10] C. H. Lee, C. N. Chang and J. A. Jiang, "Evaluation of ground potential rises in a commercial building during a direct lightning stroke using CDEGS," *IEEE Transactions on Industry Applications*, vol. 51, no. 6, pp. 4882-4888, 2015.
DOI: https://doi.org/10.1109/TIA.2015.2399618

[11] C. Tian, Y. Zhang, L. Cai, J. Wang, S. Huang and Y. Wang, "Lightning transient characteristics of a 500-kV substation grounding grid," IEEE 2011 7th Asia-Pacific International Conference on Lightning, pp. 711-715, 2011.
DOI: https://doi.org/10.1109/APL.2011.6110219

[12] W. Ruan, S. Fortin, F. P. Dawalibi, F. Grange and S. Journet, "Transient ground potential rises at a nuclear fusion experimental power plant hit directly by a lightning strike," *IEEE 2011 7th Asia-Pacific International Conference on Lightning*, pp. 192-197, 2011.
DOI: https://doi.org/10.1109/APL.2011.6111102

[13] "IEEE Recommended Practice for Determining the Electric Power Station Ground Potential Rise and Induced Voltage from a Power Fault," in *IEEE Std 367-2012 (Revision of IEEE Std 367-1996)* , vol., no., pp.1-168, 2012.
DOI: https://doi.org/10.1109/IEEESTD.2012.6203485

[14] S. Sekioka, K. Mori, N. Fukazu, K. Aiba and S. Okabe, "Study on simulation model of lightning strike to ground to calculate lightning overvoltages in residence," *IEEE Transactions on Power Delivery*, vol. 25, no. 2, pp. 970-978, 2010.
DOI: https://doi.org/10.1109/TPWRD.2009.2035626

[15] IEEE Standards Association, "IEEE Guide for Safety in AC Substation Grounding," IEEE std 80-2000, 2000.
DOI: https://doi.org/10.1109/IEEESTD.2015.7109078

[16] International Electrotechnical Commission, "Protection Against Lightning - Part 1: General Principles," zinoglobal.com.
URL: http://zinoglobal.com/wp-content/uploads/2019/12/IEC-62305-1.pdf (accessed 12 Sept, 2019)

[17] International Electrotechnical Commission, "Protection Against Lightning - Part 2: Risk Management," zinoglobal.com.
URL http://zinoglobal.com/wp-content/uploads/2019/12/IEC62305-2.pdf (accessed 12 Sept, 2019)

[18] International Electrotechnical Commission, "Protection Against Lightning - Part 3: Physical Damage to Structures and Life Hazard," zinoglobal.com.
URL: http://zinoglobal.com/wp-content/uploads/2019/12/IEC-62305-3.pdf (accessed 12 Sept, 2019)

[19] International Electrotechnical Commission, "Protection Against Lightning - Part 4: Electrical and Electronic Systems Within Structures," zinoglobal.com.
URL: http://zinoglobal.com/wp-content/uploads/2019/12/IEC-62305-4.pdf (accessed 12 Sept, 2019)

[20] J. He, B. Zhang and R. Zeng, "Maximum limit of allowable ground potential rise of substation grounding system," *IEEE Transactions on Industry Applications*, vol. 51, no. 6, pp. 5010-5016, 2015.
DOI: https://doi.org/10.1109/TIA.2015.2427121

[21] R. Zeng, X. Gong, J. He, B. Zhang and Y. Gao, "Lightning impulse performances of grounding grids for substations considering soil ionization," *IEEE Transactions on Power Delivery*, vol. 23, no. 2, pp. 667-675, 2008.
DOI: https://doi.org/10.1109/TPWRD.2007.915194

[22] International Electrotechnical Commission, "Low-voltage surge protective devices - Part 11: Surge protective devices connected to low-voltage power systems - Requirements and test methods," zinoglobal.com.
URL: http://zinoglobal.com/wp-content/uploads/2019/12/IEC-61643-11.pdf (accessed 12 Sept, 2019)